Journal of Environmental Management 132 (2014) 188–196

Contents lists available at ScienceDirect

Journal of Environmental Management

journal homepage: www.elsevier.com/locate/jenvman

Sorptive removal of arsenate using termite mound

Fekadu Fufa [a,*], Esayas Alemayehu [b], Bernd Lennartz [a]

[a] Faculty of Agricultural and Environmental Sciences, Rostock University, Justus-Von-Liebig-Weg 6, 18055 Rostock, Germany
[b] Jimma Institute of Technology, Jimma University, Ethiopia

ARTICLE INFO

Article history:
Received 7 February 2013
Received in revised form
5 October 2013
Accepted 19 October 2013
Available online

Keywords:
Termite mound
Arsenate
Sorption
Adsorbent dissolution
Kinetics

ABSTRACT

Long-term consumption of arsenic results in severe and permanent health damages. The aim of the study was to investigate arsenate (As(V)) sorption capacity of termite mound (TM), containing mainly silicon, aluminum, iron and titanium oxides, under batch adsorption setup. The pattern of As(V) removal with varying contact time, solution pH, adsorbent dose, As(V) concentration and competing anions was investigated. Dissolution of the adsorbent was insignificant under the equilibrium conditions. Equilibrium was achieved within 40 min of agitation time. Kinetic data of As(V) adsorption followed well the pseudo-second order equation ($R^2 > 0.99$). High As(V) removal efficiency ($\sim$ 99%) was observed over a pH range $\sim$ 3–$\sim$ 10, which is of great importance in the practical application. The Freundlich and Dubinin–Radushkevich isotherms well described ($R^2 > 0.99$, $\chi^2 \sim 0.05$) the equilibrium As(V) adsorption, giving a coefficient of adsorption 1.48 $mg^{1-1/n}L^{1/n}/g$ and a saturation capacity 13.50 mg/g respectively. The obtained value of mean sorption energy ($E_{DR} = 13.32$ kJ/mol) suggested the chemisorption mechanism of As(V) adsorption on TM. The removal of As(V) was significantly decreased in the presence of phosphate ions. The As(V) loaded adsorbent was successfully regenerated using NaOH solution with insignificant loss of metals. Therefore, the results of the study demonstrated that TM could be considered as a promising adsorbent for the treatment of As(V) in drinking water.

1. Introduction

Arsenic is one of the chemicals of greatest health concern in some natural waters, particularly groundwater. It is a toxic and carcinogenic metalloid that severely damages human health. Arsenic is introduced into the aqueous environment from natural as well as anthropogenic sources. High arsenic concentrations in excess of the WHO guideline, 10 μg/L (WHO, 2006), have been found in different parts of the world (Foster, 2003), including Ethiopia (Rango et al., 2010). Long-term consumption of arsenic contaminated drinking water results in severe and permanent health damages, such as dermal lesion, skin cancer, bladder and lung cancers (WHO, 2006). Thus, health problems associated with arsenic contaminated drinking groundwater have motivated researchers to develop different removal methods. Many treatment technologies, such as lime, alum or iron coagulation, chemical oxidation, adsorption, reverse osmosis, membrane filtration, activated alumina or carbon, solvent extraction, ion exchange, ligand exchangers obtained by Zr (IV), Fe (III), Mo(VI), La(III), and Al(III) onto cation exchange and chelating resins, and metal oxides based adsorbents and many others have been investigated for the removal of arsenic (Awual et al., 2012; and the references cited therein; Mohan and Pittman, 2007). Most of the treatment techniques are expensive. As a result, researchers have been working to explore low cost and easy-to-handle removal technologies (Zha et al., 2013). Among numerous arsenic treatment technologies developed, adsorption is receiving increasing attention because of simplicity, cheaper pollution control method, ease of operation and handling, sludge free operation and possibility of regeneration (Han et al., 2012; Kundu and Gupta, 2006). However, some of the limitations of the adsorption method are the harmful dissolution of adsorbents and the need for pH adjustment (Han et al., 2012; Li et al., 2012a).

Mounds are built by termites which substantially modify the physicochemical properties of soil and have the ability to change mineralogy of clay (Jouquet et al., 2002; Semhi et al., 2008). Geochemical analysis done by Aufreiter et al. (2001) shows that mound soil contains relatively high aluminum. Furthermore, Abe and Wakatsuki (2010) observe generally greater iron content in the mound than in the neighboring soil and the influence of termites on the forms and composition of free sesquioxides. The increase in the content of titanium is also observed in the mounds (Sako et al., 2009). Iron, aluminum and titanium as well as their oxides are incorporated into other materials to enhance the

* Corresponding author. Tel.: +49 177 2828 422; fax: +49 381 498 3122.
E-mail address: fekaduff2010@gmail.com (F. Fufa).

0301-4797/$ – see front matter © 2013 Elsevier Ltd. All rights reserved.
http://dx.doi.org/10.1016/j.jenvman.2013.10.018

adsorption efficiency of the materials. However, termite mound (TM), containing mainly silicon, aluminum, iron and titanium oxides, has not been evaluated for the removal of arsenate (As(V)). Therefore, the objectives of this study were: (1) to examine the As(V) sorption capacity of TM under batch adsorption setup, (2) to assess the As(V) adsorption pattern with respect to varying contact time, solution pH, adsorbent dose, initial As(V) concentration, and concentration of competing anions, and (3) to investigate the reusability of the As(V) loaded adsorbent and loss of metals under batch desorption conditions.

2. Materials and methods

2.1. Adsorbent

TMs are widely distributed and abundant in nature (Jouquet et al., 2002; López-Hernández et al., 2006; Semhi et al., 2008). In the southern and western parts of Ethiopia, average TM abundance is found to be 12 mounds per hectare (Abdulrahman, 1990; Tilahun et al., 2012). In the western part of the country, in 8 districts of east and west Wallaga Zones, infestation of mound building termites causes destruction of crops, wooden houses and natural resources (OADB, 2001). According to the study conducted by Tilahun et al. (2012), the average mound soil mass is computed to be 58.9 t/ha. Six separate samples of mound soil were collected from six TMs in the surroundings of Gimbi, west Welega Zone, Oromia Regional National State, western Ethiopia. The rocks of the sampling area are Precambrian formations comprising a wide range of sedimentary, volcanic and intrusive rocks that have been metamorphosed to varying degrees (Tadesse et al., 2003). The six samples were mixed thoroughly on an equal proportion to make a composite sample, and dried afterwards at room temperature in a laboratory. Particle size analysis of the composite sample was performed according to the American Society for Testing and Materials (ASTM D 422) and soil textural classification system (Liu and Evett, 2003). The dried sample was crushed, sieved to particle size <0.075 mm and stored in airtight plastic bottles for later batch adsorption experiments.

2.1.1. Characterization

2.1.1.1. Chemical composition. The oxide and elemental compositions of TM were analyzed using X-Ray Fluorescence (XRF) spectrometry and inductively coupled plasma, ICP, spectrometer (Thermo Scientific iCAP 6300 ICP, Thermo Fischer Scientific, Cambridge, UK), respectively. The total carbon, total nitrogen and total sulfur contents were determined using Elementar Vario EL analyser (Elementar Analysensysteme GmbH, Hanau, Germany) according to DIN ISO 10694 and 13878 (DIN ISO 10 694, 1996; DIN ISO 13878, 1998).

2.1.1.2. pH and point of zero charge. The pH of the adsorbent was measured using a Microprocessor pH 196 meter (pH 196, WTW, Germany) in a 1:10 TM/water ratio according to the standard method (Appel and Ma, 2002). The pH of the point of zero charge (pH_{PZC}) was determined by potentiometric titration method described in Appel et al. (2003).

2.1.1.3. Specific area. The BET surface area of TM of particle < 0.075 mm was measured using Micromeritics ASAP 2010 (USA) by N_2 adsorption method after degassing. The Micromeritics ASAP 2010 provides high quality surface area and equipped with the software that allows performing automatic analysis as well as collecting analysis reports.

2.1.2. Solubility

The dissolution of TM under the equilibrium experimental conditions (solution pH: ~7, shaking speed: 200 rpm, contact time: 60 min and temperature: 24.6 °C) was examined through the analysis of the concentrations of the elements in the supernatant solution using ICP spectrometer. The anions in the supernatant solution were analyzed using ion chromatography (Metrohm AG, Switzerland).

2.2. Chemicals

All the chemicals used were analytical grade reagent from Merck, Darmstadt, Germany. The stock solution of As(V) was prepared dissolving $Na_2HAsO_4.7H_2O$ in deionized water. Solutions of bicarbonate, carbonate, chloride, nitrate, sulfate and phosphate anions were prepared from their respective potassium salts. The pH of the solution was adjusted using 0.1 M NaOH and/or 0.1 M HCl.

2.3. As(V) adsorption

A series of duplicate batch adsorption experiments were conducted at room temperature (23.5–25.5 °C) in acid washed polyethylene plastic bottles with blank (only with TM) and control (only with As(V)) experiments. A 500 mL aqueous solution containing a known As(V) concentration and a desired TM dose was shaken at 200 rpm on a horizontal shaker (SM25, Edmund Bühler 7400 Tübinger, Germany) for a predetermined contact time, and the solid was separated afterwards by filtration using 0.45 μm acetate filter paper (Sartorius Stedim Biotech GmbH, Germany). Then, As(V) concentration in the filtrate was analyzed on inductively coupled plasma, ICP, spectrometer (Thermo Scientific iCAP 6300 ICP, Thermo Fischer Scientific, Cambridge, UK). The average of the duplicate measurements was reported. In all experiments, particle size of < 0.075 mm was used.

2.3.1. Effect of contact time

In order to determine the equilibrium contact time at which the adsorption completed, the agitation time was varied from 0 to 60 min. The 0.21 and 2 mg/L As(V) aqueous solutions of pH ~ 7 separately shaken with 2 g/L TM at 200 rpm for a predetermined contact time. The amount of As(V) adsorbed per unit mass of TM, and the percentage of As(V) adsorbed were computed respectively using Eqs. (1) and (2) given below:

$$q_t = \left(\frac{C_0 - C_t}{M}\right) \times V \quad (1)$$

$$A\% = \left(\frac{C_0 - C_t}{C_0}\right) \times 100 \quad (2)$$

where, q_t (mg/g) is the amount of As(V) adsorbed at any time, t (min); $A(\%)$ is the percentage of As(V) adsorbed; C_0 (mg/L) is initial As(V) concentration; C_t (mg/L) is concentration of As(V) in the aqueous phase at any time, t; V (L) is volume of the aqueous solution; and M (g) is mass of TM used in the experiment.

2.3.2. Effect of pH

The effect of solution pH was investigated to determine the optimum pH for maximum adsorption of As(V) over the initial pH range ~ 3–~ 11 by allowing 2 g/L TM to adsorb 0.21 mg/L As(V) in the aqueous solution.

2.3.3. Effect of adsorbent dose

To determine the optimum dose required for the reduction of As(V) to a desired level, different doses ranging from 0.1 to 25 g/L TM were separately added into a 0.21 mg/L As(V) aqueous solution of pH ~ 7 and shaken at 200 rpm for 60 min.

2.3.4. Effect of initial concentration

The effect of initial concentration was examined varying the concentration from 0.21 to 10 mg/L As(V) while maintaining the solution pH at ~ 7, dose at 2 g/L TM, shaking speed at 200 rpm and contact time at 60 min.

2.3.5. Effect of co-existing anions

The influence of co-existing ions at different concentration levels ranging from 10 to 500 mg/L was examined in such a way that each ion separately and in a mixture added to a container of 500 mL solution of 0.21 mg/L As(V) of pH ~ 7 with 2 g/L TM and shaken at 200 rpm for 60 min.

2.3.6. Groundwater

A sample of groundwater was collected from a hand pump well in the Main Campus of Jimma University, Oromia Regional National State, western Ethiopia. The analyzed physicochemical characteristics of the sample were: pH (7.87), conductivity (1215 μS/cm), total hardness (645.56 mg/L), carbonate (nil), bicarbonate (764.94 mg/L), chloride (3.41 mg/L), nitrate (0.2 mg/L), sulfate (3.94 mg/L), phosphate (0.12 mg/L), fluoride (7.56 mg/L), calcium (10.64 mg/L), magnesium (3.65 mg/L), sodium (278 mg/L) and As (< 0.001 mg/L). The water sample was spiked with 0.21 mg/L As(V) and treated afterwards with 2 g/L TM to evaluate the As(V) adsorption efficiency of the adsorbent under natural groundwater conditions.

2.4. Desorption

To evaluate the regenerative property of the As(V) loaded TM, 0.21 mg/L As(V) in the aqueous solution was initially allowed to adsorb on 2 g/L TM at pH ~ 7 shaking at 200 rpm for 60 min. After adsorption, the solid was separated by filtration and dried at 105 °C for 24 h in an oven. Desorption was conducted shaking the dried As(V) loaded TM at 200 rpm for 60 min in 500 mL solution of 0.1 and 0.2 M NaOH separately. Besides, the pH of deionized water was adjusted to ~ 5 to assess the release of As(V) ion from the As(V) loaded adsorbent for safe disposal of the spent TM at pH ≤ 5. The amount of As(V) ion desorbed from the spent adsorbent into the solution was then determined by quantifying the concentration of As(V) in the supernatant solution. The dissolution of TM during the regeneration process using 0.2 M NaOH solution was examined via the analysis of the concentrations of the elements in the supernatant solution.

3. Results and discussion

3.1. Adsorbent

3.1.1. Characterization

3.1.1.1. Chemical composition. The analyzed chemical compositions of the adsorbent (wt%) were: SiO_2 (27.43), Al_2O_3 (22.83), Fe_2O_3 (26.08), TiO_2 (8.86), MgO (0.83), Na_2O (< 0.01), K_2O (0.23), CaO (< 0.01), MnO (0.25), P_2O_3 (0.35), SO_3 (0.33) and loss on ignition (11.29). Measured values (wt%) of total C, S and N were 2.30, 0.28 and 0.40, respectively. The elemental compositions (wt%) were: Si (15.07), Fe (12.67), Al (6.35), Ti (1.50), Na (< 0.01), Mg (< 0.01), K (< 0.01), Cr (0.01), Mn (0.21), P (0.35), and the concentrations of trace elements, such as Hg, Pb, As, Ni, and Cd were below the detection limit.

3.1.1.2. pH and point of zero charge. The pH of the adsorbent measured in water was found to be 5.10. The pH_{PZC} determined by potentiometric titration method was 7.96, which is within the range of the pH_{pzc} of the mixture of Fe, Al and Si oxides, 5.5 to 8.3 (Brown et al., 1999), and similar with the pH_{pzc} of TM ($pH_{pzc} = 7.8$) investigated for the adsorptive removal of Pb(II) (Abdus-Salam and Itiola, 2012).

3.1.1.3. Specific area. The BET surface area of the adsorbent of particle size < 0.075 mm was found to be 28.40 m^2/g. Results of particle size analysis showed that majority of the particles was in the range of 0.075–2.00 mm with mean particle size (d_{50}) of 0.51 mm.

3.1.2. Solubility

The concentrations of the elements (wt%) in the supernatant solution obtained under the equilibrium experimental conditions were: Si (3.00×10^{-3}), Fe (3.45×10^{-3}), Al (4.97×10^{-3}), As (bdl), Ni (7.33×10^{-6}), Cd (bdl), Cr (7.00×10^{-6}), Pb (bdl), F^- (6.67×10^{-6}), Cl^- (9.45×10^{-3}), NO_3^- (1.13×10^{-3}) and SO_4^{2-} (1.12×10^{-2}), where bdl is below the detection limit. The results indicated that TM dissolution was insignificant, and the concentrations of the elements released under the equilibrium experimental conditions were significantly lower than their maximum permissible levels in drinking water (WHO, 2006). This indicated that no toxic sludge was generated by TM. Therefore, TM could be used safely as an adsorbent for As(V) removal.

3.2. As(V) adsorption

3.2.1. Effect of contact time

The plots of the amount of As(V) adsorbed versus contact time are given in Fig. 1. The results showed that As(V) adsorption was fast within the first 5 min of agitation time and slow afterwards until equilibrium. For example, the amount of As(V) adsorbed per unit gram of TM within 5 min contact time was ~ 0.63 mg/g for 2 mg/L As(V) in the solution. The rapid uptake of As(V) within the first 5 min agitation time was due to the presence of competent active adsorbing sites on the surface of the adsorbent at the initial stage of the contact time. Equilibrium time was achieved within 40 min, and the equilibrium time appeared to be independent of the initial concentration. However, in order to be sure that the adsorption was completed, the agitation time was maintained at 60 min for further studies.

3.2.1.1. Kinetic. The analysis of the adsorption kinetic data applying kinetic models is useful to predict the mechanism of adsorption and the potential rate-limiting step. The adsorption kinetic of a system can be explained by the pseudo-second order equation (Ho and McKay, 1999) when the removal of an adsorbate from aqueous solution increases during the initial agitation time, and followed by a slow increase until the equilibrium time. Accordingly, the linear form of the pseudo-second order equation (Eq. (3)) was employed to evaluate the kinetic of As(V) adsorption on TM (Ho and McKay, 1999). Besides, the intraparticle diffusion model (Eq. (4)) based on the theory proposed by Weber and Morris (Zha et al., 2013; Zhao et al., 2012) was applied to examine the diffusion mechanism of the adsorbate.

$$\frac{t}{q_t} = \frac{1}{k_2 q_e^2} + \frac{1}{q_e}(t) \tag{3}$$

$$q_t = k_p t^{0.5} + C \tag{4}$$

where q_t (mg/g) is the amount of As(V) adsorbed per unit mass of TM at any time, t (min); q_e (mg/g) is the calculated equilibrium capacity; k_2 (g/(mg.min)) is the equilibrium rate constant based on the pseudo-second order equation; k_p (mg/(g.$min^{0.5}$)) is the intraparticle diffusion rate constant; and C (mg/g) is the intercept of the intraparticle diffusion model.

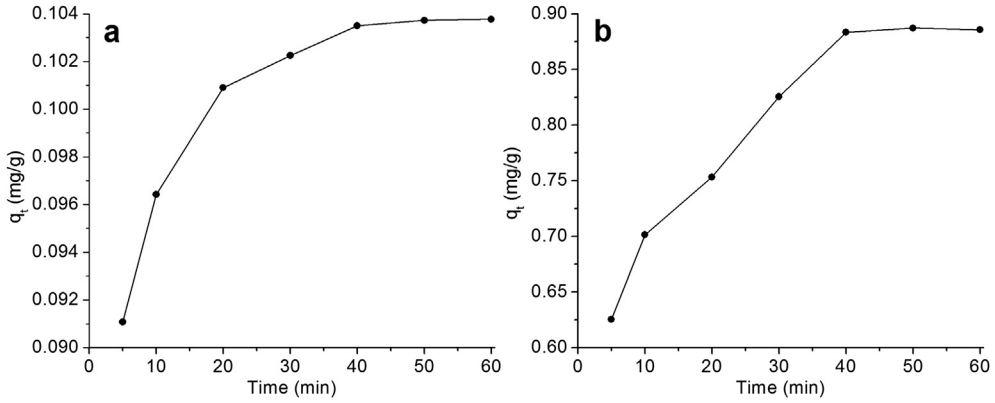

Fig. 1. Effect of contact time on As(V) adsorption: (a) 0.21 mg/L As(V) and (b) 2 mg/L As(V).

3.2.1.2. Analysis of kinetic data. The pseudo-second order rate constant (k_2), calculated equilibrium capacity ($q_{e,\mathrm{cal}}$) and adsorption affinity ($V_0 = k_2 q_e^2$) were computed from the plot of t/q_t versus t (not shown). Numerical values of parameters of the pseudo-second order equation along with the standard deviation (SD) are given in Table 1. The computed values of k_2, $q_{e,\mathrm{cal}}$ and V_0 revealed the decrease in k_2 value (11.071–0.313 g/(mg.min)), and the increase in the values of $q_{e,\mathrm{cal}}$ (0.105–0.881 mg/g) and V_0 (0.123–0.275 mg/(g.min)) with the increase in the concentration of As(V) from 0.21 to 2 mg/L. The decrease in the rate of adsorption, k_2, with the increase in the solute concentration could indicate the higher the As(V) concentration in the solution the faster the adsorption (Camacho et al., 2010). The value of the adsorption affinity, V_0, is important in providing information about the adsorption rate, particularly at the beginning of the adsorption process (Li et al., 2012b). According to the result obtained, the value of V_0 increased with the increase in the solute concentration which indicated that the adsorption affinity increased with the increase in the initial concentration. The plots of t/q_t versus t were straight lines (not shown) with the coefficients of determination, $R^2 > 0.99$. In addition, the values of the modeled equilibrium capacities, $q_{e,\mathrm{cal}}$, were comparable to the experimental equilibrium capacities, $q_{e,exp}$. Thus, the kinetic of As(V) adsorption on TM well described by the pseudo-second order equation, implying that the rate-limiting step could be chemical adsorption involving valence forces through the sharing or exchange of electrons between adsorbent and adsorbate (Ho and McKay, 1999). Similar results are obtained in the removal of As(V) from water using magnetite Fe_3O_4-reduced graphite oxide-MnO_2 nanocomposites (Luo et al., 2012) and magnesia-loaded fly ash cenospheres and manganese-loaded fly ash cenospheres (Li et al., 2012a).

Table 1
Pseudo-second order and intraparticle diffusion parameters of As(V) adsorption on TM.

Model	Parameter	As(V) concentration (mg/L)			
		0.21		2.0	
		Value	SD	Value	SD
Pseudo-second order	$q_{e,exp}$ (mg/g)	0.104	6.03×10^{-4}	0.881	4.51×10^{-3}
	$q_{e,\mathrm{cal}}$ (mg/g)	0.105	9.58×10^{-4}	0.937	7.13×10^{-2}
	k_2 [g/(mg.min)]	11.071	6.12×10^{-1}	0.313	1.31×10^{-2}
	V_o [mg/(g.min)]	0.123	5.67×10^{-4}	0.275	1.25×10^{-2}
	R^2	0.9999		0.998	
Intraparticle diffusion	k_p [mg/(g.min$^{0.5}$)]	0.002	5.85×10^{-5}	0.049	7.84×10^{-2}
	C (mg/g)	0.089	2.21×10^{-3}	0.537	6.24×10^{-1}
	R^2	0.8569		0.9445	

The plots of the intraparticle diffusion model for the adsorption of As(V) on TM are given in Fig. 2. The parameters obtained from the model along with the SD are given in Table 1. The plots indicate that the As(V) adsorption process involved only two stages, suggesting that the external diffusion may be the rapid process compared to the relatively slow process of the intraparticle diffusion stage. The plots did not pass through the origin further indicating that the intraparticle diffusion was not the only rate-controlling diffusion mechanism (Zha et al., 2013). Therefore, the adsorption of As(V) and its kinetics could be the cumulative result of the external diffusion transport of As(V), the intrarparticle diffusion of the ions and the adsorption of As(V) ions by the active sites on TM (Theydan and Ahmed, 2012). Table 1 shows that the value of the diffusion rate, k_p, was higher at higher concentration, signifying that the diffusion rate was faster at higher concentration level than at lower concentration (Yan et al., 2008; Zhao et al., 2012). The result is similar to previous observations (Zha et al., 2013; Zhao et al., 2012).

3.2.2. Effect of pH and mechanism of As(V) adsorption

The removal of As(V) by TM at varying initial solution pH is graphically presented in Fig. 3. The result showed that TM had high adsorption capacity over a wide pH range. It was observed that ~ 99% of As(V) removal was achieved between pH ~ 3 and ~9, and the percentage of removal decreased to ~ 97% at pH ~ 10. The As(V) adsorption significantly decreased from ~ 97 to ~ 32% with the increase in the solution pH from ~ 10 to ~ 11. The sharp decrease in the removal of As(V) beyond pH ~ 10 could be due to the increase in the negative charge site on the surface of the adsorbent (Mostafa et al., 2011). The high As(V) removal over a wide pH range could be attributed to the pH buffering capacity of TM. The pH buffering capacity of the adsorbent can be explicable by its high content of Al and Fe oxides that are amphoteric in nature (Cornell and Schwertmann, 1996; Guo et al., 2007; Shriver et al., 1994), and the insignificant composition of basic metallic oxides. Besides, SO_3 and P_2O_3 content of TM (*Sub section 3.1.1.1*), which are covalent oxides, release H_3O^+ in the aqueous solution by binding H_2O molecules, thereby decreasing the pH of the medium (Shriver et al., 1994). Thus, iron and aluminum oxides along with the covalent oxides could decrease the equilibrium pH of the solution in synergy when the initial solution pH is in the alkaline range. The pH dependency of As(V) removal can be explained also considering the pH_{pzc} of the adsorbent which was found to be 7.96. When the pH < pH_{pzc}, As(V) would be adsorbed on the adsorbent surface by the columbic attraction, whereas when the pH > pH_{pzc}, the adsorption of As(V) could take place through a ligand exchange reaction (Ayoob and Gupta, 2009). The stability of As(V) species depend on pH (Zhang and Itoh, 2005), and the stable As(V) species

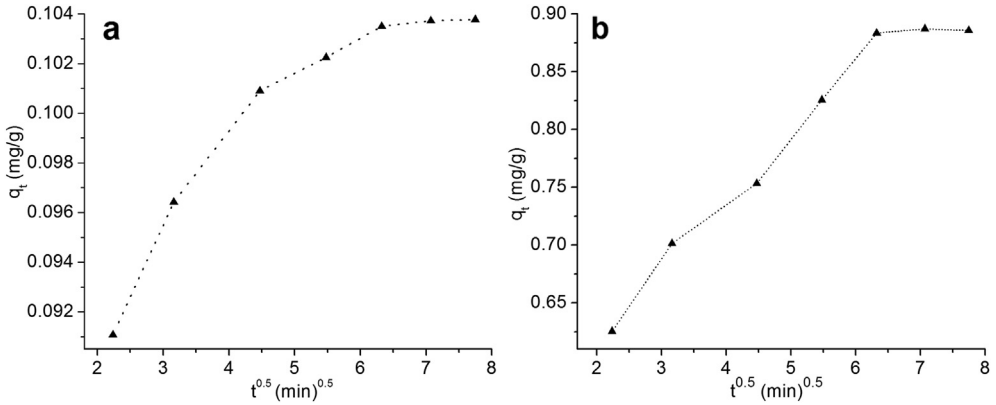

Fig. 2. Intraparticle diffusion plots of As(V) adsorption on TM: (a) 0.21 mg/L As(V) and (b) 2 mg/L As(V).

present at each pH are: H_3AsO_4 (0–2), $H_2AsO_4^-$ (2–7), $HAsO_4^{2-}$ (7–12) and AsO_4^{3-} (12–14). The As(V) used in the present study was in form of $HAsO_4^{2-}$. Thus, the plausible mechanisms involved in the adsorption of As(V) from aqueous solution can be proposed using Eqs. (5) and (6) (Li et al., 2012a).

$$\equiv MOH_2^+ + H_2AsO_4^- \leftrightarrow \equiv MOH_2 \cdots H_2AsO_4 \quad (5)$$

$$\equiv MOH_2^+ + HAsO_4^{2-} \leftrightarrow (\equiv MOH_2)_2 \cdots HAsO_4 \quad (6)$$

where M represents metals, such as Si, Fe, Al and Ti. Moreover, the measured equilibrium pHs were between 5.0 and 6.31 (data were not shown) when the initial pHs of the solution were between 4 and 10, which could be as well due to the buffering effect of TM. The result is similar to previous observations (Li et al., 2012a; Zha et al., 2013).

3.2.3. Effect of adsorbent dose

The pattern of As(V) adsorption with varying TM dose is presented in Fig. 4. The result showed that the As(V) loading capacity (the amount of As(V) adsorbed per unit mass of TM) progressively decreased from 1.81 to 0.01 mg/g with the increase in the adsorbent dose from 0.50 to 25 g/L. The progressive decrease in the loading capacity was possibly due to the lower ratio of As(V) ions to the available active binding sites with the increase in the mass of the adsorbent (Thole, 2011). On the contrary, the efficiency of As(V) removal increased rapidly from ~ 86 to ~ 98% as the adsorbent dose increased from 0.10 to 2 g/L, and increased slowly to a maximum of ~ 99% when the dose increased from 2 to 25 g/L TM. The increase in the removal percentage with the increase in the adsorbent dose can be attributed to the increase in the number of the adsorption sites as the amount of adsorbent increased (Thole, 2011). Consequently, the ratio of the number of active binding sites to the constant As(V) concentration in the solution increased, and thus resulting the increase in the percent of As(V) adsorbed. It was observed that 2 g/L TM reduced 0.21 mg/L As(V) to 0.004 mg/L, which is below the WHO guideline value, 0.01 mg/L, of arsenic in the drinking water. Hence, the 2 g/L TM was considered as an optimum dose and used in the subsequent experiments.

3.2.4. Effect of initial concentration

The plot of As(V) removal as a function of varying the initial concentration is given in Fig. 5. It was noticed that the amount of As(V) adsorbed progressively increased from 0.01 to 2.73 mg/g with the increase in the initial concentration from 0.21 to 10 mg/L As(V). The increase in the adsorption capacity with the increase in the initial concentration of the solute could be attributed to the availability of more As(V) ions for adsorption at higher concentration on poorly reachable sites with weak sorption energy (Kumar et al., 2011). Consequently, the energetically less favorable sites become involved in the adsorption process with increasing As(V) concentration in the aqueous solution (Chutia et al., 2009). However, the

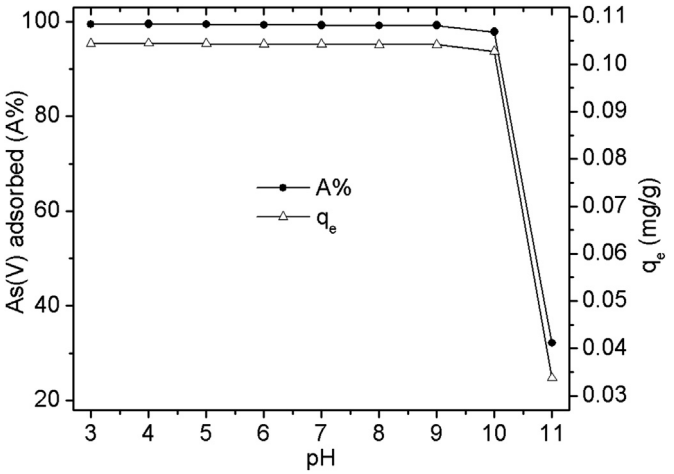

Fig. 3. Effect of pH on the adsorption of As(V) by TM.

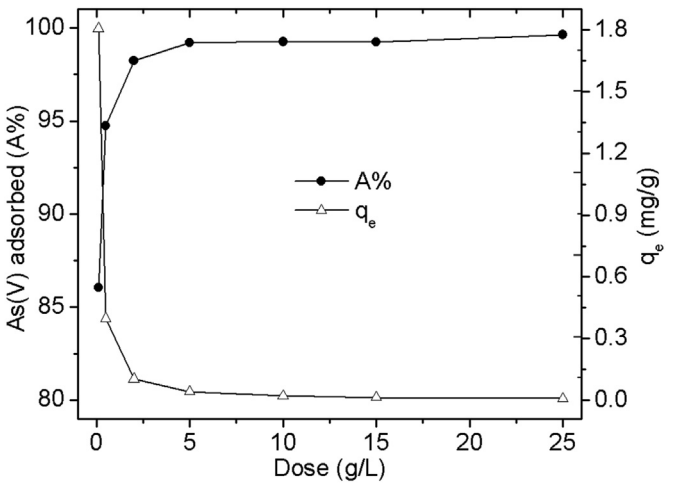

Fig. 4. Effect of adsorbent dose on As(V) removal by TM.

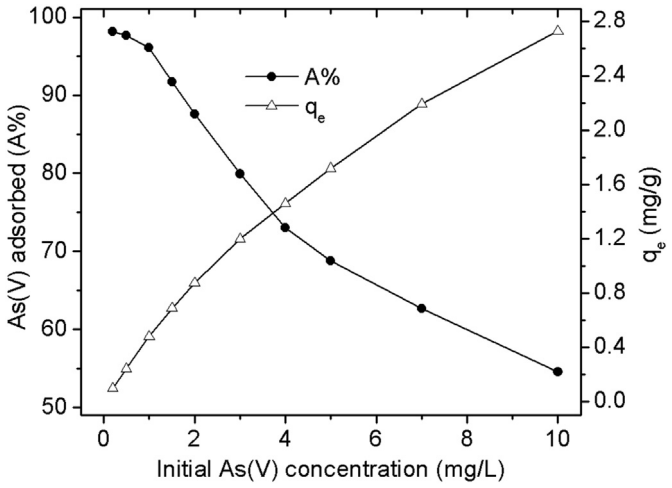

Fig. 5. Effect of initial concentration on the removal of As(V) by TM.

percentage of As(V) removal decreased from 98.18 to 54.59% with the increase in the initial concentration from 0.21 to 10 mg/L As(V). This can be explained in that at high-level As(V) concentrations the number of available adsorption sites became fewer, thus resulting in a relatively lower percentage of As(V) removal (Tiwari and Lee, 2012). Overall, the results indicated that As(V) removal by TM was dependent on the initial concentration over the range 0.21–10 mg/L As(V).

3.2.4.1. Isotherm. In this study, the equilibrium isotherm data set of As(V) adsorption was evaluated applying nonlinear equations of the Langmuir, the Freundlich and the Dubinin–Radushkevich (D–R) isotherms expressed in Eqs. (7)–(9), respectively. The three isotherm models are widely used in the modeling of water and waste water treatment (Chutia et al., 2009; Kundu and Gupta, 2006; Li et al., 2012b). The Freundlich isotherm assumes multilayer adsorption of a solute on the heterogeneous surface sites of a solid, whereas the Langmuir isotherm predicts monolayer adsorption process over the homogeneous surface sites. The D–R equation is commonly used to estimate the mean sorption energy of the adsorption process and the nature of adsorption as physical or chemical (Kundu and Gupta, 2006; Zhao et al., 2012).

$$q_e = \frac{Q_{\max} b C_e}{(1 + bC_e)} \tag{7}$$

$$q_e = K_F C_e^{1/n} \tag{8}$$

$$q_e = q_m \exp\left(-K_{DR}\varepsilon^2\right) \tag{9}$$

$$\varepsilon = RT\ln(1 + 1/C_e) \tag{10}$$

where C_e (mg/L) is the concentration of As(V) in the aqueous phase at equilibrium; q_e (mg/g) is the amount of As(V) adsorbed at equilibrium per unit mass of TM; Q_{max} (mg/g) is the adsorption capacity based on the Langmuir equation; b (L/mg) is the Langmuir constant; K_F ($mg^{1-1/n}$ $L^{1/n}$/g) is the adsorption coefficient based on the Freundlich equation; $1/n$ is the adsorption intensity based on the Freundlich equation; q_m (mol/g) is the molar adsorption capacity based on the D–R equation; K_{DR} (mol^2/kJ^2) is the activity coefficient related to the mean sorption energy; ε (mol^2/kJ^2) is the Polanyi potential; R (kJ/(mol.K)) is the gas constant; and T (K) is the temperature of the equilibrium experiment.

Two error quantifiers, the coefficient of determination and the chi-squared test statistic, were used to evaluate the goodness of fit of a model to the observed equilibrium isotherm data. The chi-squared test statistic, χ^2, is computed using Eq. (11) as described in Meenakshi et al. (2008).

$$\chi^2 = \sum \left(q_e - q_{e,\text{cal}}\right)^2 / q_e \tag{11}$$

where $q_{e,cal}$ (mg/g) is the equilibrium capacity obtained by calculating from the model; and q_e (mg/g) is the experimental equilibrium capacity. If data from the model are similar to the experimental data, χ^2 will be a small number, whereas if they differ, χ^2 will be a bigger number (Meenakshi et al., 2008). The value of standard deviation, SD, for each parameter along with the χ^2 and R^2 values for each isotherm model is presented in Table 2.

3.2.4.2. Analysis of isotherm data. The isotherm plots of the equilibrium adsorption of As(V) on TM are given in Fig. 6. Values of the equilibrium constants computed from nonlinear equations of the isotherms are presented in Table 2. From the evaluation of the fitting criteria, it was clear that the Freundlich and the D–R isotherms demonstrated higher coefficients of determination, $R^2 > 0.99$, and lower chi-square statistic, $\chi^2 \sim 0.05$, values. Thus, both the Freundlich and the D–R isotherm equations well described the equilibrium isotherm data set of As(V) adsorption, giving respectively a coefficient of adsorption 1.48 $mg^{1-1/n}L^{1/n}$/g, and a saturation capacity 13.50 mg/g, which are indicatives of the relative adsorption capacity of the adsorbent. The fitting of the equilibrium data to the Freundlich isotherm indicated the multilayer adsorption of As(V) on the heterogeneous surface sites of TM. The nature of adsorption isotherm can be predicted by evaluating the essential characteristic of the Langmuir isotherm expressed in terms of a dimensionless constant separation factor, R_L. The separation factor was computed by $R_L = 1/(1 + bC_0)$ (Gupta and Ghosh, 2009), where C_0 (mg/L) is the initial As(V) concentration; and b (L/mg) is the Langmuir constant. The adsorption process is irreversible if $R_L = 0$, favorable if $0 < R_L < 1$, linear if $R_L = 1$ and unfavorable if $R_L > 1$. The values of R_L computed for As(V) adsorption on TM were from 0.08 to 0.80 with decreasing in value at high level of initial concentration. The obtained values of R_L are within the range 0–1, signifying the favorable equilibrium adsorption of As (V) on TM (Kundu and Gupta, 2006). The magnitude of the adsorption intensity, $1/n$, computed from the Freundlich equation can suggest the type of isotherm. In that, the adsorption is favorable when $0 < 1/n < 1$, irreversible when $1/n = 1$ and unfavorable when $1/n > 1$ (Gao et al., 2013). The value of $1/n$ obtained for the equilibrium adsorption of

Table 2
Isotherm parameters of the equilibrium adsorption of As(V) on TM.

Freundlich isotherm			Langmuir isotherm			D–R isotherm		
Parameter	Value	SD	Parameter	Value	SD	Parameter	Value	SD
K_F [$(mg^{1-1/n}L^{1/n})$/g]	1.480	6.23×10^{-2}	Q_{max} (mg/g)	2.929	1.33	q_m (mg/g)	13.504	9.95×10^{-1}
$1/n$	0.398	3.22×10^{-2}	b (L/mg)	1.233	1.06	E_{DR} (kJ/mol)	13.316	2.54×10^{-1}
R^2	0.997		R^2	0.960		R^2	0.993	
χ^2	0.046		χ^2	2.782		χ^2	0.052	

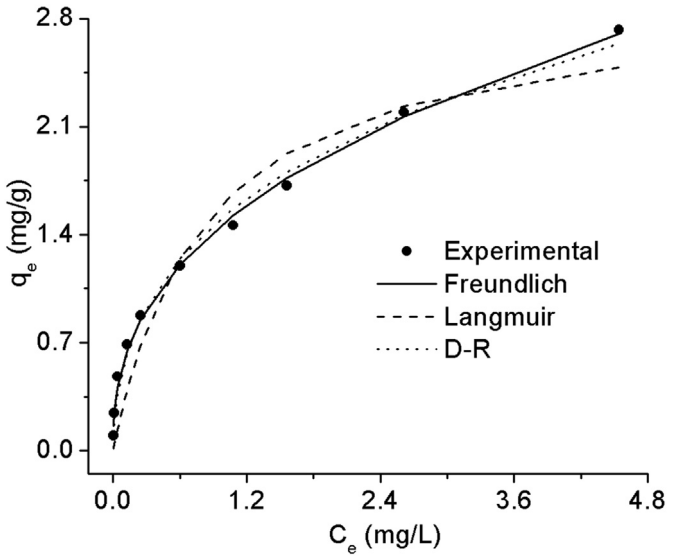

Fig. 6. Isotherms of equilibrium adsorption of As(V) on TM.

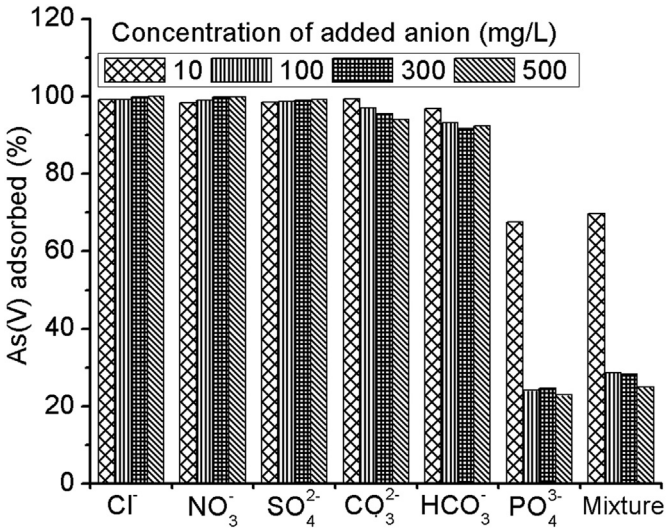

Fig. 7. Effect of co-existing anions on the removal of As(V) by TM.

As(V) was 0.398. Therefore, As(V) was adsorbed favorably on TM as the numerical value of $1/n$ is in the range 0–1, which is similar to the observation made by Zhao et al. (2012) for the adsorption of As(V) on Al_{13}-modefied montmorillonite.

The mean sorption energy, E_{DR} (kJ/mol), of equilibrium As(V) adsorption was computed from the D–R isotherm using the equation $E_{DR} = (-2K_{DR})^{-0.5}$ as given in Gupta and Ghosh (2009). The E_{DR} value of an adsorption system predicts the mechanism of the adsorption process of a solute on a solid adsorbent. The adsorption process is of physical nature if $0 < E_{DR} < 8$ kJ/mol, and considered to be chemical adsorption if 8 kJ/mol $< E_{DR} <$ 16 kJ/mol (Kundu and Gupta, 2006). In the present study, the value of E_{DR} computed for the equilibrium adsorption of As(V) was 13.32 kJ/mol (Table 2). The obtained E_{DR} value was in the range of chemisorption process, implying that TM had high affinity for As(V) ion (Zhao et al., 2012). Thus, the observed high E_{DR} value indicated that chemisorption should be the dominant plausible mechanism for As(V) adsorption on TM (Gupta and Ghosh, 2009; Kundu and Gupta, 2006). Similar observations are made previously by Gupta and Ghosh (2009) and Zhao et al. (2012) for As(V) adsorption.

3.2.5. Effect of co-existing anions

Natural inorganic anions in water could be reactive toward the adsorbent surface, thereby influencing the adsorptive removal of As(V). In order to assess the potential applicability of TM as an adsorbent for As(V) removal from natural water, adsorption efficiency was evaluated as a function of various concentrations of bicarbonate, carbonate, chloride, nitrate, phosphate, sulfate and their mixture. The influences of the presence of these anions separately and in a mixture in the solution on the efficiency of As(V) adsorption on TM are shown in Fig. 7. The results showed that phosphate, among the six anions, caused the greatest decrease in the removal of As(V). The result is in agreement with the previous studies (Chowdhury and Yanful, 2010; Tuutijärvi et al., 2012). The high interference of phosphate on As(V) adsorption on TM was expected, as phosphate and arsenate have similar structure and chemical behavior. As a result, both ions compete for specific adsorption sites, thereby phosphate at high level of concentrations significantly reducing As(V) adsorption (Tuutijärvi et al., 2012). Besides, both phosphate and arsenate are inner-sphere complex anions behaving identically toward the active binding sites on the adsorbent surface (Zhu et al., 2009). In general, the adsorption of As(V) decreased by increasing the initial phosphate to As(V) concentration ratio, as was the case in this study that is the As(V) concentration was kept constant at 0.21 mg/L while the initial concentration of phosphate increased from 10 to 500 mg/L sequentially. It was also observed that As(V) adsorption was sharply decreased in the presence of the mixture of all the six anions in the same aqueous solution, which could be ascribed to the capacity of phosphate to overshadow the buffering abilities of the other anions as phosphate forms inner-sphere complex. However, phosphate is absent or very rarely occurs at high level of concentrations in the groundwater (Rango et al., 2010), so its effect on As(V) removal would not be a problem. Bicarbonate and carbonate, which commonly exist with elevated arsenic in the groundwater, had insignificant effect on the As(V) adsorption over the concentration range 10–500 mg/L. Earlier study reported that the presence of carbonate species had little effect on the As(V) adsorption by ferrihydrite (Fuller et al., 1993). Chloride, nitrate and sulfate had no influence on As(V) adsorption under the studied concentration ranges, and the result is similar to previous observation (Li et al., 2012b). Both nitrate and chloride form outer-sphere complexes (Tuutijärvi et al., 2012), and thus they would not directly compete for the same adsorption sites with As(V). In a previous study (Maji et al., 2007), where sulfate, which can form either outer or inner-sphere complex, and As(V) were present simultaneously, 1000 mg/L sulfate did not show interference on 0.5 mg/L As(V) removal by laterite soil. The overall influence of the studied co-existing anions on the As(V) removal by TM thus can be summarized in the order phosphate ≈ mixture > bicarbonate ≈ carbo nate > sulfate ≈ nitrate ≈ chloride.

3.2.6. Groundwater

The competence of TM under natural groundwater conditions was evaluated using 0.21 mg/L As(V) spiked groundwater sample of pH 7.87. The obtained result demonstrated that the 0.21 mg/L As(V) in the spiked groundwater sample was reduced to 0.0043 mg/L, which is below the WHO guideline value of arsenic in drinking water. Therefore, TM could be a potential geomaterial for adsorptive removal of arsenic from drinking water without pH adjustment.

3.3. Desorption

The effect of pH on As(V) removal by TM (Fig. 3) indicated that As(V) adsorption drastically decreased in the pH > 10, so As(V)

desorption from the spent TM was considered under higher alkaline conditions. Based on this, the batch desorption of As(V) from the As(V) loaded TM was conducted using 500 mL solution of 0.1 and 0.2 M NaOH separately under experimental conditions identical to the equilibrium batch adsorption conditions. It was found that the percentages of As(V) desorbed by 0.1 and 0.2 M NaOH solution were 80.72 and 98.08% respectively. It was also observed that no detectable As(V) was released from the As(V) loaded TM at pH $\sim$ 5. Thus, the As(V) loaded TM can be either regenerated or safely disposed at pH $\leq$ 5 without causing environmental pollution. The loss of metals under the regeneration conditions was investigated through the analysis of the elements in the supernatant solution obtained using 0.2 M NaOH. Accordingly, the analysis results (wt%) were: Fe (2.80×10^{-2}), Al (1.39), Ni (6.56×10^{-5}), Cd (2.22×10^{-6}), Cr (1.29×10^{-4}) and Pb (5.89×10^{-4}). The results indicated that the regeneration of the spent TM using 0.2 M NaOH solution did not cause significant dissolution of the adsorbent. Hence, the decrease in the adsorption efficiency of the regenerated spent TM could be expected very minimal. However, further investigation should be considered to determine the adsorption efficiency and the exact life cycle of the regenerated TM.

4. Conclusion

The present study investigated the As(V) adsorption behavior of TM under various batch adsorption experimental parameters. The rate of As(V) uptake by the adsorbent was fast, which is the required characteristics of an adsorbent. The high As(V) removal demonstrated by the adsorbent over the natural groundwater pH range is essential for the practical application of TM without pH adjustment. The values of the coefficient of adsorption and the saturation capacity, which are the indicators of the relative adsorption capacity, obtained respectively from the fitted models, the Freundlich and the D–R isotherms, indicated the potential of TM to adsorb As(V) with an acceptable dose and contact time. The favorable adsorption of As(V) on TM was signified by the obtained values of the separation factor and the adsorption intensity. The fitting of the kinetic data of As(V) adsorption to the pseudo-second order and the computed value of the mean sorption energy were suggestive of the dominant chemisorption mechanism of As(V) adsorption on the adsorbent. The negligible effect of the competing anions that commonly occur with elevated levels of As(V) in the groundwater as well as the competence TM demonstrated under natural groundwater physicochemical characteristics to reduce As(V) to below the required level signified the strong affinity of the adsorbent for As(V). The stability that TM demonstrated under the present batch adsorption equilibrium and regeneration conditions was a desirable characteristic overcoming the harmful dissolution problem. Therefore, the results of the study provided fundamental information for further evaluation of TM in the practical application for the treatment of As(V) under domestic conditions.

Acknowledgments

The first author is thankful to the Ethiopian Engineering Capacity Building Program (ECBP) and the German Academic Exchange Service (DAAD) for their financial support. The first author would like also to thank Mr. Reinhard Eckelt of Leibniz-Institut für Katalyse der Unversität Rostock e.v and the institute for the characterization of the adsorbent.

References

Abdulrahman, A., 1990. Foraging Activity and Control of Termites in Western Ethiopia. PhD thesis. London University, London.

Abdus-Salam, N., Itiola, A.D., 2012. Potential application of termite mound for adsorption and removal of Pb(II) from aqueous solutions. J. Iran. Chem. Soc. 9, 373–382.

Abe, S.S., Wakatsuki, T., 2010. Possible influence of termites (*Macrotermes bellicosus*) on forms and composition of free sesquioxides in tropical soils. Pedobiologia 53, 301–306.

Appel, C., Ma, L., 2002. Concentration, pH, and surface charge effects on cadmium and lead sorption in three tropical soils. J. Environ. Qual. 31, 581–589.

Appel, C., Ma, L.Q., Dean Rhue, R., Kennelley, E., 2003. Point of zero charge determination in soils and minerals via traditional methods and detection of electroacoustic mobility. Geoderma 113, 77–93.

Aufreiter, S., Mahaney, W.C., Milner, M.W., Huffman, M.A., Hancock, R.G.V., Wink, M., Reich, M., 2001. Mineralogical and chemical interactions of soil eaten by chimpanzees of the Mahale Mountains and Gombe Stream National Parks, Tanzania. J. Chem. Ecol. 27, 285–311.

Awual, M.R., Shenashen, M.A., Yaita, T., Shiwaku, H., Jyo, A., 2012. Efficient arsenic(V) removal from water by ligand exchange fibrous adsorbent. Water Res. 46, 5541–5550.

Ayoob, S., Gupta, A.K., 2009. Performance evaluation of alumina cement granules in removing fluoride from natural and synthetic waters. Chem. Eng. J. 150, 485–491.

Brown Jr., G.E., Henrich, V.E., Casey, W.H., Clark, D.L., Eggleston, C., Felmy, A., Goodman, D.W., Grätzel, M., Maciel, G., McCarthy, M.I., Nealson, K.H., Sverjensky, D.A., Toney, M.F., Zachara, J.M., 1999. Metal oxide surfaces and their interactions with aqueous solutions and microbial organisms. Chem. Rev. 99, 77–174.

Camacho, L.M., Torres, A., Saha, D., Deng, S., 2010. Adsorption equilibrium and kinetics of fluoride on sol-gel-derived activated alumina adsorbents. J. Colloid Inteface Sci. 349, 307–313.

Chowdhury, S.R., Yanful, E.K., 2010. Arsenic and chromium removal by mixed magnetite-maghemite nanoparticles and the effect of phosphate on removal. J. Environ. Manage. 91, 2238–2247.

Chutia, P., Kato, S., Kojima, T., Satokawa, S., 2009. Arsenic adsorption from aqueous solution on synthetic zeolites. J. Hazard. Mater. 162, 440–447.

Cornell, R.M., Schwertmann, U., 1996. The Fe Oxides-structure, Properties, Reactions, Occurrence and Uses. VCH, New York.

DIN ISO 10 694, 1996. Bodenbeschaffenheit-Bestimmung von organischem Kohlenstoff und Gesamtkohlenstoff nach trockener Verbrennung (Elementaranalyse). Beuth, Berlin.

DIN ISO 13878, 1998. Bodenbeschaffenheit - Bestimmung des Gesamt-Stickstoffs durch trockene Verbrennung (Elementaranalyse). Beuth, Berlin.

Foster, A.L., 2003. Spectroscopic investigations of arsenic species in solid phases. In: Welch, A.H., Stollenwerk, K.G. (Eds.), Arsenic in Groundwater, Geochemistry and Occurrence. Kluwer, Boston.

Fuller, C.C., Davis, J.A., Waychunas, G.A., 1993. Surface chemistry of ferrihydrite: part 2. kinetics of arsenate adsorption and coprecipitation. Geochim. Cosmochim. Acta 57, 2271–2282.

Gao, Z.P., Yu, Z.F., Yue, T.L., Quek, S.Y., 2013. Adsorption isotherm, thermodynamics and kinetics studies of polyphenols separation from kiwifruit juice using adsorbent resin. J. Food Eng. 116, 195–201.

Guo, H., Stüben, D., Berner, Z., 2007. Removal of arsenic from aqueous solution by natural siderite and hematite. Appl. Geochem. 22, 1039–1051.

Gupta, K., Ghosh, U.C., 2009. Arsenic removal using hydrous nanostructure iron(III)-titanium(IV) binary mixed oxide from aqueous solution. J. Hazard. Mater. 161, 884–892.

Han, D.S., Batchelor, B., Park, S.H., Abdel-Wahab, A., 2012. As(V) adsorption onto nanoporous titania adsorbents (NTAs): effects of solution composition. J. Hazard. Mater. 229-230, 273–281.

Ho, Y.S., McKay, G., 1999. Pseudo-second order model for sorption processes. Process. Biochem. 34, 451–465.

Jouquet, P., Mamou, L., Lepage, M., Velde, B., 2002. Effect of termites on clay minerals in tropical soils: fungus-growing termites as weathering agents. Eur. J. Soil Sci. 53, 521–528.

Kumar, E., Bhatnagar, A., Kumar, U., Sillanpää, M., 2011. Defluoridation from aqueous solutions by nano-alumina: characterization and sorption studies. J. Hazard. Mater. 186, 1042–1049.

Kundu, S., Gupta, A.K., 2006. Arsenic adsorption onto iron oxide-coated cement (IOCC): regression analysis of equilibrium data with several isotherm models and their optimization. Chem. Eng. J. 122, 93–106.

Li, Q., Xu, X., Cui, H., Pang, J., Wei, Z., Sun, Z., Zhai, J., 2012a. Comparison of two adsorbents for the removal of pentavalent arsenic from aqueous solutions. J. Environ. Manage. 98, 98–106.

Li, R., Li, Q., Gao, S., Shang, J.K., 2012b. Exceptional arsenic adsorption performance of hydrous cerium oxide nanoparticles: part A. adsorption capacity and mechanism. Chem. Engin. J. 185-186, 127–135.

Liu, C., Evett, J.B., 2003. Soil Properties-testing, Measurement, and Evaluation. Banta Book Company, USA.

López-Hernández, D., Brossard, M., Fardeau, J.-C., Lepage, M., 2006. Effect of different termite feeding groups on P sorption and P availability in African and South American savannas. Biol. Fert. Soils 42, 207–214.

Luo, X., Wang, C., Luo, S., Dong, R., Tu, X., Zeng, G., 2012. Adsorption of As(III) and As(V) from water using magnetite Fe_3O_4-reduced graphite oxide-MnO_2 nanocomposites. Chem. Eng. J. 187, 45–52.

Maji, S.K., Pal, A., Pal, T., 2007. Arsenic removal from aqueous solutions by adsorption on laterite soil. J. Environ. Sci. Health A Tox. Hazard. Subst. Environ. Eng. 42, 453–462.

Meenakshi, S., Sundaram, C.S., Sukumar, R., 2008. Enhanced fluoride sorption by mechanochemically activated kaolinites. J. Hazard. Mater. 153, 164–172.
Mohan, D., Pittman Jr., C.U., 2007. Arsenic removal from water/wastewater using adsorbents-a critical review. J. Hazard. Mater. 142, 1–53.
Mostafa, M.G., Chen, Y.-H., Jean, J.-S., Liu, C.-C., Lee, Y.-C., 2011. Kinetics and mechanism of arsenate removal by nanosized iron oxide-coated perlite. J. Hazard. Mater. 187, 89–95.
OADB, 2001. Phase II: Integrated Pilot Project for Termite Control in 8 Districts of East and West Wallaga Zone, Oromia. Oromia Agricultural Development Bureau (OADB), Finfinne.
Rango, T., Bianchini, G., Beccaluva, L., Tassinari, R., 2010. Geochemistry and water quality assessment of central Main Ethiopian Rift natural waters with emphasis on source and occurrence of fluoride and arsenic. J. Afr. Earth Sci. 57, 479–491.
Sako, A., Mills, A.J., Roychoudhury, A.N., 2009. Rare earth and trace element geochemistry of termite mounds in central and northeastern Namibia: mechanisms for micro-nutrient accumulation. Geoderma 153, 217–230.
Semhi, K., Chaudhuri, S., Clauer, N., Boeglin, J.L., 2008. Impact of termite activity on soil environment: a perspective from their soluble chemical components. Int. J. Environ. Sci. Techn 4, 431–444.
Shriver, D.F., Atkins, P.W., Langford, C.H., 1994. Inorganic Chemistry. Oxford University Press, Oxford.
Tadesse, S., Milesi, J.-P., Deschamps, Y., 2003. Geology and mineral potential of Ethiopia: a note on geology and mineral map of Ethiopia. J. Afr. Earth Sci. 36, 273–313.
Theydan, S.K., Ahmed, M.J., 2012. Adsorption of methylene blue onto biomass-based activated carbon by $FeCl_3$ activation: equilibrium, kinetics, and thermodynamic studies. J. Anal. Appl. Pyrol 97, 116–122.
Thole, B., 2011. Defluoridation kinetics of 200°C calcined bauxite, gypsum, and magnesite and breakthrough characteristics of their composite filter. J. Fluor. Chem. 132, 529–535.
Tilahun, A., Kebede, F., Yamoah, C., Erens, H., Mujinya, B.B., Verdoodt, A., Ranst, E.V., 2012. Quantifying the masses of *Macrotermes subhyalinus* mounds and evaluating their use as a soil amendment. Agri. Ecosys. Environ. 157, 54–59.
Tiwari, D., Lee, S.M., 2012. Novel hybrid materials in the remediation of groundwaters contaminated with As(III) and As(V). Chem. Eng. J. 204–206, 23–31.
Tuutijärvi, T., Repo, E., Vahala, R., Sillanpää, M., Chen, G., 2012. Effect of competing anions on arsenate adsorption onto maghemite nanoparticles. Chin. J. Chem. Eng. 20, 505–514.
WHO, 2006. Guidelines for Drinking Water Quality, First addendum to third ed., vol. 1. Recommendations, Switzerland, Geneva.
Yan, L.-g., Shan, X.-q., Wen, B., Owens, G., 2008. Adsorption of cadmium onto Al_{13}-pillared acid-activated montmorillonite. J. Hazard. Mater. 156, 499–508.
Zha, F., Huang, W., Wang, J., Chang, Y., Ding, J., Ma, J., 2013. Kinetic and thermodynamic aspects of arsenate adsorption on aluminum oxide modified palygorskite nanocomposites. Chem. Eng. J. 215–216, 579–585.
Zhang, F.-S., Itoh, H., 2005. Iron oxide-loaded slag for arsenic removal from aqueous system. Chemosphere 60, 319–325.
Zhao, S., Feng, C., Huang, X., Li, B., Niu, J., Shen, Z., 2012. Role of uniform pore structure and high positive charges in the arsenate adsorption performance of Al_{13}-modified montmorillonite. J. Hazard. Mater. 203–204, 317–325.
Zhu, H., Jia, Y., Wu, X., Wang, H., 2009. Removal of arsenic from water by supported nano zero-valent iron on activated carbon. J. Hazard. Mater. 172, 1591–1596.